Dissipative solitons and vortices in polariton Bose-Einstein condensates

Elena A. Ostrovskaya,[1] Jasur Abdullaev,[1] Anton S. Desyatnikov,[1] Michael D. Fraser,[2] and Yuri S. Kivshar[1]
[1]*Nonlinear Physics Centre, Research School of Physics and Engineering, The Australian National University, Canberra, ACT 0200, Australia*
[2]*National Institute of Informatics, Tokyo, Japan*
(Received 7 May 2012; published 23 July 2012)

We examine spatial localization and dynamical stability of Bose-Einstein condensates of exciton polaritons in microcavities under the condition of off-resonant spatially inhomogeneous optical pumping both with and without a harmonic trapping potential. We employ the open-dissipative Gross-Pitaevskii model for describing an incoherently pumped polariton condensate coupled to an exciton reservoir, and reveal that spatial localization of the steady-state condensate occurs due to the effective self-trapping created by the polariton flows supported by the spatially inhomogeneous pump, regardless of the presence of the external potential. A ground state of the polariton condensate with repulsive interactions between the quasiparticles represents a dynamically stable bright dissipative soliton. We also investigate the conditions for sustaining spatially localized structures with nonzero angular momentum in the form of single-charge vortices.

DOI: 10.1103/PhysRevA.86.013636 PACS number(s): 03.75.Kk, 03.75.Lm, 71.35.Lk, 71.36.+c

I. INTRODUCTION

Since the first observation of spontaneous exciton-polariton condensation in a microcavity [1], significant effort in this vigorous field has been directed towards understanding the properties of superfluid flow in the novel nonequilibrium polariton superfluid [2–5]. Recently, considerable attention was drawn to the controlled creation of spatially localized collective excitations of the exciton-polariton Bose-Einstein condensate (BEC). Most notably, moving bright solitons have been predicted [6] and observed in a pioneering proof-of-principle experiment [8]. The properties of polariton solitons, superior to those of optical solitons in semiconductor cavity lasers, namely, the picosecond response times and large nonlinearities, suggest that polariton BEC can offer novel functionalities for information-processing devices [7]. The bright solitons observed in [8] require a resonant excitation regime at nonzero in-plane momentum to make use of the dispersion properties of the lower-polariton branch that allow the polaritons to have a negative effective mass. In this regime, strong repulsive interactions between the quasiparticles can be balanced by the effective dispersion to achieve localization. A similar mechanism for spatial localization via effective mass management is well explored for atomic BECs in optically induced band-gap structures [9]. In the absence of the spectral gap, however, localization by means of effective mass management is only possible in one spatial dimension. The question whether localization of polariton BEC with repulsive interactions can occur in the regime of spontaneous condensation at zero in-plane momentum (positive effective mass) and nonresonant excitation, remains open.

In this paper we examine, both analytically and numerically, formation and dynamical stability of a steady-state BEC of exciton polaritons in microcavities in the presence of a spatially localized (Gaussian) optical pump. By employing the open-dissipative Gross-Pitaevskii model [10] describing an incoherently pumped BEC coupled to the exciton reservoir and successfully used in theoretical description of a number of significant experiments (see, e.g., [2,4]), we analyze the mechanisms for creating and sustaining two-dimensional spatially localized structures, such as dissipative solitons and vortices. In addition to the trap-free case, we analyze the structure of the localized states with the addition of a harmonic external potential that can be created, e.g., by engineered stress of the microcavity [11]. In the latter case, the localization of the repulsive polariton BEC is due to both the harmonic confinement and the inhomogeneous pump, in contrast to the case of a trapped atomic BEC with a positive scattering length in thermal equilibrium.

We show, analytically and numerically, that, even in the absence of external potentials localization of the steady-state polariton BEC occurs due to the effective self-trapping created by the polariton flows due to spatially inhomogeneous off-resonant optical pumping. Spatial localization of the condensate occurs due to the internal balance of superfluid density flows which is identical to that responsible for supporting dissipative "antisolitons" in optical systems. Such localization of continuously self-defocusing solitons occurs despite the repulsive interactions between the quasiparticles, and is analogous to optical gain-guiding effect [12,13] in its reliance on continuous pumping. Thus a *ground state of the polariton BEC* represents a *dissipative soliton* which is spatially localized and dynamically stable, regardless of the presence of the external potential. A harmonic trapping potential dramatically modifies the structure of the steady state due to the competition with the spatially inhomogeneous pump (see Fig. 1).

A single vortex created in a localized steady-state BEC by phase imprinting is similarly supported by the continuous inhomogeneous pump as a spatially localized *dissipative vortex soliton*. Akin to a vortex line in a trapped atomic BEC with a positive scattering length, it is dynamically unstable [14]. In the absence of potential, a vortex line spirals out of the polariton condensate and the condensate restores to its ground steady state. We show that the addition of fabricated (i.e., nonrotating) harmonic potential modifies the threshold of the optical pumping required to sustain a steady state with an angular momentum and leads to the possibility of a long-term survival of the vortex.

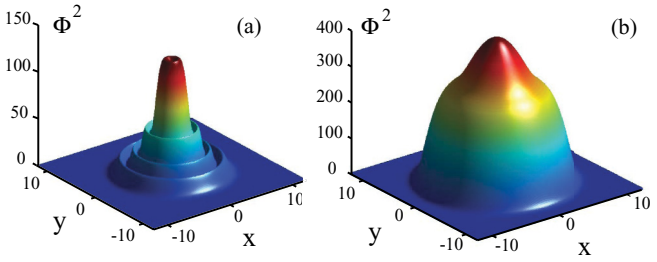

FIG. 1. (Color online) Typical steady-state density of a harmonically trapped polariton condensate in the regime of (a) narrow and (b) wide pump (see text).

II. MODEL

We consider a spontaneously formed exciton-polariton BEC ($k_{||} = 0$, lower-polariton branch) under the continuous-wave nonresonant excitation. The model first suggested in [10] consists of a mean-field equation for the polariton condensate wave function and a rate equation for the inhomogeneous density of the exciton reservoir. We write it here in the form used in [4]:

$$i\hbar\frac{\partial\Psi}{\partial t} = \left[-\frac{\hbar^2}{2m}\nabla_\perp^2 + V(\vec{r},t) + i\frac{\hbar}{2}(Rn_R - \gamma_c)\right]\Psi,$$
$$\frac{\partial n_R}{\partial t} = -(\gamma_R + R|\Psi|^2)n_R(\vec{r},t) + P(\vec{r}), \tag{1}$$

where $V(\vec{r},t) = U(\vec{r}) + g_c|\Psi|^2 + g_R n_R(\vec{r},t)$. Here Ψ is the condensate wave function, n_R is the exciton reservoir density, $P(\vec{r})$ is the inhomogeneous optical pump, and $U(\vec{r})$ is the external potential. The critical parameters defining the condensate dynamics are the loss rates of the polaritons γ_c and reservoir excitons γ_R, the stimulated scattering rate R, condensate coupling to the reservoir g_R, and the coefficient g_c quantifying the nonlinear interaction of polaritons. In what follows, we will consider a radially symmetric external trapping potential $U(r) = U_0^2 r^2$, where $U_0 = 0$ in a trap-free case.

The model can be rewritten in dimensionless form by using the following characteristic scaling units of time, energy, and length:

$$T = 1/\gamma_c, \quad E = \hbar\gamma_c, \quad L = \sqrt{\frac{\hbar}{m_{LP}\gamma_c}}, \tag{2}$$

where m_{LP} is the lower-polariton effective mass. Here, we choose the parameters close to those of the experimental setup of [4], with $m_{LP} = 10^{-4}m_e$, $g_c = 6\times10^{-3}$ meV μm^2, $g_R = 2g_c$, $\gamma_c = 0.33$ ps^{-1}, $\gamma_r = 1.5\gamma_c$, and $R = 0.01$ μm^2 ps^{-1}. In what follows we use and plot the dimensionless (normalized) variables and parameters.

We recall that, in the spatially homogeneous case, one can estimate the threshold pumping power at which the condensate appears in the system, as described in [10]. This threshold is approximately determined by the values of parameters for which stimulated gain equals loss:

$$P_{\rm th} \approx \frac{\gamma_R\gamma_c}{R}. \tag{3}$$

The ratio of the polariton n_c to exciton reservoir n_R densities in the steady homogeneous state can then be defined as

$$\frac{n_c}{n_R} = \frac{\gamma_c}{\gamma_R}(\bar{P} - 1), \tag{4}$$

where normalized pump is defined as $\bar{P} = P/P_{\rm th} \geqslant 1$. In general, even in a spatially inhomogeneous case, the typical dynamical behavior of the model equations (1) displays rapid transition to the steady state of the polariton BEC for $\bar{P} > 1$.

Below we consider the properties of the steady state supported by an inhomogeneous (Gaussian) optical pump, $P(r) = P_0\exp(-r^2/\sigma^2)$, with or without an additional trapping potential. The spot size of the optical pump is considered to be small compared to the size of the sample, so that the local density approximation [15] is not applicable.

III. STEADY STATE OF THE CONDENSATE

A. Theory

For a general continuous-wave pump, the condensate wave function in the steady state can be looked for in the following general form: $\Psi = \psi(x,y)\exp(-i\mu t)$, where μ is the energy (chemical potential) of the steady state. If both the external potential and the pump are radially symmetric, we can rewrite the model system in polar coordinates $(x,y) \to (r,\theta)$ and reduce the problem to finding radially symmetric steady states $\psi(x,y) = \psi(r)\exp(im\theta)$, where m is the phase winding number [16] (topological charge of a vortex), and the ground state corresponds to $m = 0$.

The steady-state wave function $\psi(r)$ obeys the following stationary equation:

$$\nabla_r^2\psi - 2V(r)\psi - i\left(Rn_R^0 - \gamma_c\right)\psi + 2\mu\psi = 0, \tag{5}$$

where $\nabla_r^2 = \partial^2/\partial r^2 + (1/r)\partial/\partial r - m^2/r^2$, $V(r) = g_c|\psi|^2 + g_R n_R^0 + U(r)$, and the steady-state reservoir density is found from Eqs. (1) as

$$n_R^0 = \frac{P(r)}{\gamma_R + R|\psi|^2}. \tag{6}$$

All physical parameters in Eq. (5) are dimensionless, and under the adopted scaling (2), $\gamma_c = 1$. However, we formally retain this parameter in subsequent formulas.

The stationary wave function can be further separated into the real amplitude and phase: $\psi(r) = \Phi(r)\exp[i\phi(r)]$. Following the analysis suggested in [17] for the generalized complex Ginzburg-Landau equation, we can obtain asymptotic behavior of amplitude and phase of the condensate wave function. In the absence of a trapping potential, $U(r) = 0$, the requirement of spatial localization, $P(r) \to 0$, $|\psi(r)| \to 0$, imposed on both the pump and the condensate wave function at large r leads to the following asymptotic behavior of the amplitude and the phase at $r \to \infty$:

$$\Phi(r) \sim A\,\exp(-p_- r), \quad \phi(r) \sim B + p_+ r, \tag{7}$$

where $p_\pm = [(\mu^2 + \gamma_c^2/4)^{1/2} \pm \mu]^{1/2}$, and A, B are real constants. This asymptotic behavior shows that the condensate decays slower than the pump field, and therefore the spatial profile of the condensate will significantly differ from that of the pump.

Conversely, at $r \to 0$, the asymptotic behavior is found to be

$$\Phi(r) \sim C r^{|m|} \exp(-q_- r^2), \quad \phi(r) \sim q_+ r^2, \tag{8}$$

where $q_- = (1/2)(1+|m|)^{-1}[V(0)-\mu]$ and $q_+ = (1/4)(1+|m|)^{-1}[Rn_R^0(0)-\gamma_c]$, and for the ground state $C = \Phi(0) \equiv \Phi_0$. For $V(0) < \mu$, the second derivative of the amplitude changes sign at $r = 0$, i.e., the condensate displays a central "dip" in its density profile and acquires a ring shape, as seen in Fig. 1(a).

The presence of the harmonic trap $U(r) = U_0^2 r^2$ dramatically modifies the asymptotic behavior of the condensate wave function for $r \to \infty$ [18], so that

$$\begin{aligned} \Phi(r) &\sim A \exp\left[-U_0^2 r^2 + (\mu - 1/2)\ln(2U_0 r)\right], \\ \phi(r) &\sim B + \gamma_c \ln(2U_0 r). \end{aligned} \tag{9}$$

The asymptotic behavior of a trapped polariton BEC at $r \to 0$ is described by Eq. (8).

For a spatially localized (e.g., Gaussian) pump, $P(r)$, the spatial localization of the condensate in the absence of an added trapping potential is counterintuitive. Indeed, the effective potential $V(r)$ formed by the repulsive nonlinearity (due to polariton scattering) and interaction with the exciton reservoir is *antitrapping*. Therefore the balance of nonlinearity and dispersion responsible for nonlinear localization in conservative condensate systems cannot be achieved. Physically, the existence of the spatially localized steady state of the polariton condensate can be understood by examining the internal flows of the dissipative polariton superfluid, analogous to the Pointing vector flows in dissipative optical systems [17,19]. Indeed, by defining the superfluid current density (flux) in the standard way $\vec{j} = \mathrm{Im}(\Psi^* \nabla \Psi)$, we can recast Eq. (5) in the form of coupled equations for the amplitude of the condensate wave function Φ and radial component of the stationary flux $J = j_r = n_c v_r$, where $n_c = \Phi^2(r)$ is the condensate density, and v_r is the radial component of the flow velocity $\vec{v} = (d\phi/dr)\vec{e}_r + (m/r)\vec{e}_\theta$. The equations for these variables take the following form:

$$\begin{aligned} \frac{1}{r}\frac{d}{dr}(rJ) - \left(Rn_R^0 - \gamma_c\right)\Phi^2 &= 0, \\ \nabla_r^2 \Phi - 2[V(r) - \mu]\Phi - V_J \Phi &= 0, \end{aligned} \tag{10}$$

where $V_J = J^2 \Phi^{-4} = (d\phi/dr)^2$. The first equation of the system is the continuity equation for the stationary flow with source and sink. The first term in this equation is simply the divergence of the flux, $D = \nabla \cdot \vec{j}$, which serves as a local measure of gain ($D > 0$) or loss ($D < 0$). A steady state exists if generation of the polariton superfluid via continuous pumping is balanced by its dissipation. This condition can be formulated in terms of the flux as follows [19]:

$$\int_0^\infty D(r) r\, dr = 0. \tag{11}$$

Remarkably, this condition can be satisfied *regardless of the sign of the nonlinear interactions* in the systems, i.e., for both repulsive (as in the case of polaritons) and attractive nonlinearities. The nonlinearity affects the energy (chemical potential) of the steady state and its spatial extent according to Eqs. (7) and (9). We note that nonlinear eigenstates for a very similar dynamical one-dimensional system with linear loss and spatially localized gain and without additional external potential were found in [13]. The key feature of our system is similar: for the given parameters of gain and loss, the chemical potential, μ, is unique.

The second equation in (10) highlights the composition of the effective potential supporting the condensate wave function as its eigenstate with the corresponding eigenvalue μ. It is clear that the radial flux that exists due to the spatially inhomogeneous phase of the condensate $\phi(r) \neq \text{const}$, forms an attractive potential that can trap a spatially localized bound state even in the absence of the external trapping $U_0 = 0$. In the linear limit (i.e., for very small condensates and/or nonlinearity) this effective trapping potential due to the flux is approximately given by

$$V_J(r) \approx \frac{\gamma_c^2}{4}(\bar{P}_0 - 1)^2 r^2. \tag{12}$$

The effect of existence of the localized linear modes supported purely by the localized gain is known as "gain guiding" in optics [12].

B. Numerical results

The existence of the localized steady state of the dissipative polariton BEC with the properties described in the previous section can be demonstrated by the numerical simulation of the time-dependent model equations (1). Figure 2 shows the typical dynamical behavior and transition to the steady ground state ($m = 0$) of the polariton component for intermediate values of pumping power ($\bar{P}_0 = 3$) in the trap-free regime. In addition, from the numerical simulations we can extract and plot the following dynamical quantity:

$$\mu(t) = -\frac{1}{4}\frac{\int_S [\nabla^2|\Psi|^2 - 2|\nabla\Psi|^2 - 4V|\Psi|^2] d\vec{r}}{\int_S |\Psi|^2 d\vec{r}}, \tag{13}$$

where S is the numerical integration domain. In the steady-state limit this quantity coincides with the chemical potential of the condensate $\mu(t) \to \mu$. As can be seen from the dynamical simulations for $\bar{P} > 1$ (Fig. 2), the steady-state regime is reached quickly, and the chemical potential is well defined. Alternatively, the steady state is found by solving the stationary equation (5) by the standard one-dimensional relaxation method. The condensate wave function displays characteristic inhomogeneous amplitude and phase profile $\phi(r)$ (seen in Fig. 3) with the limiting behavior well described by Eqs. (7) and (8).

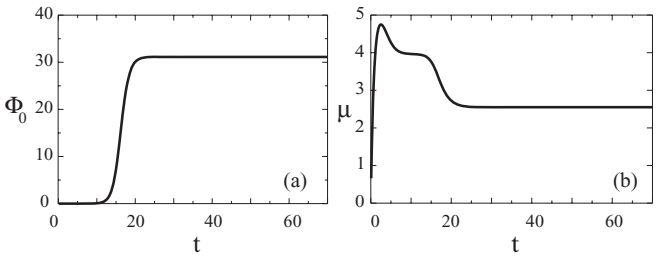

FIG. 2. Typical time evolution of (a) the condensate peak density and (b) the chemical potential for $\bar{P}_0 = 3$, without a trapping potential.

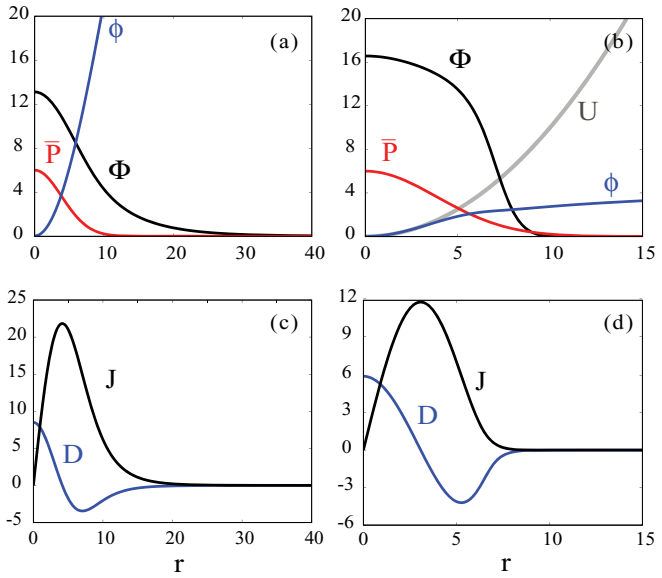

FIG. 3. (Color online) Radial profiles of the condensate ground state in (a) trap-free and (b) harmonically trapped case. Both amplitude, $\Phi(r)$, and phase, $\phi(r)$, are shown in comparison to the Gaussian pump profile $P(r)/P_{\rm th}$ with the amplitude $\bar{P}_0 = P(0)/P_{\rm th} = 6$. Profiles of the radial flux J and its divergence D (scaled up by the factor of 10) for the ground state are shown for the (c) trap-free and (d) trapped cases, respectively. The harmonic potential of the depth $U_0^2 = 0.1$ is shown in (b) by the gray curve.

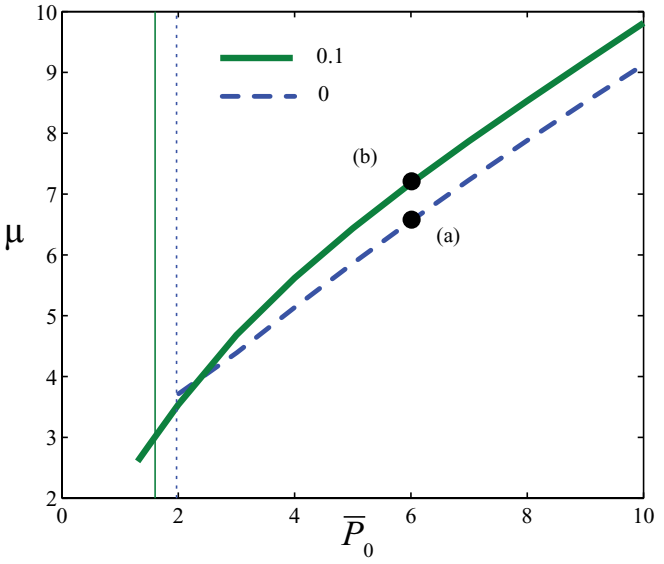

FIG. 4. (Color online) Dependence $\mu(\bar{P}_0)$ for the ground state $m = 0$ without the harmonic potential (dashed line) and in the presence of a harmonic trapping potential $U(r) = U_0^2 r^2$ with $U_0^2 = 0.1$ (solid line). Vertical dashed and solid lines indicate the cut-off values of $\bar{P}_0$ for the ground state given by the linear limit (14). Marked points (a) and (b) correspond to the condensate profiles shown in Fig. 3. The width of the pump spot is $\sigma^2 = 30$ in both cases.

From Fig. 3(c) it is seen that the inhomogeneous phase of the condensate wave function results in the nonzero flux of the polariton superfluid. Due to the spatially localized pump, the polariton superfluid is continuously generated in the core area of the steady state $D > 0$ and dissipated on its wings $D < 0$. Thus the ground state of the strongly repulsive polariton BEC is a spatially localized *dissipative soliton*. Its spatial localization is owed to the balance of the superfluid currents, and the internal structure of the currents is similar to that of a continuously "self-defocusing" dissipative "antisoliton" of the generalized complex Ginzburg-Landau equation described in [19].

The presence of a harmonic trap modifies the asymptotic behavior of the condensate and phase according to Eq. (9), as shown in Fig. 3(b). Nevertheless, the structure of the internal flow within the ground state of the condensate remains qualitatively the same, as seen in Fig. 3(d). In the trapped regime the internal flow of the polariton superfluid currents lead to significant distortions in the condensate density profile, $n_c(r)$. In particular, a wide pump with $\bar{P}_0 \gg 1$ leads to a well-pronounced central peak [shown in Fig. 1(b) for $\sigma^2 = 40$ and $\bar{P}_0 = 10$] noted in numerical simulations of a similar model of polariton BEC [20] and also hinted at in experimental observations of a trapped exciton-polariton condensate [11].

IV. TRAPPED VS TRAP-FREE REGIME

The ground $m = 0$ state of the polariton condensate can be characterized by the dependence of chemical potential μ on the parameters of the pump. In the absence of the trapping potential, this dependence is determined by the flux balance condition, and in the limit of low condensate densities the dependence of μ on the pump intensity is linear $\mu \sim \bar{P}_0 = P_0/P_{\rm th}$. In the presence of the harmonic potential, this condition is modified by the trap, as seen in Fig. 4.

For a fixed width of the pump, the cut-off value of $\bar{P}_0$ corresponds to the linear limit $|\psi| \to 0$, and deviates quite significantly from the value $\bar{P}_0 = 1$ determined by the threshold behavior (3) in the homogeneous excitation case. The linear limit is determined by the cutoff for the ground state in the effective two-dimensional (2D) potential formed by the combination of the external harmonic trap $U(r)$, repulsive potential due to the spatially localized pump $V_R(r) = g_R n_R^0$, and the internal inhomogeneous flux $V_J(r)$ given by Eq. (12). This cutoff can be estimated from the condition that the effective potential in the linear limit is trapping (attractive) rather than antitrapping (repulsive). Thus, the bound state appears in the effective potential at the value of $\bar{P}_0$ given by the positive root of the equation:

$$\bar{P}_0^2 - 2\left(1 + \frac{4g_R}{\gamma_c R}\frac{1}{\sigma^2}\right)\bar{P}_0 + \left(1 + \frac{4U_0}{\gamma_c^2}\right) = 0. \qquad (14)$$

According to this formula, for the parameters in Fig. 4, the ground state appears in the trap-free system at $\bar{P}_0 \approx 1.97$. The presence of the harmonic trap with $U_0^2 = 0.1$ lowers the threshold to $\bar{P}_0 \approx 1.61$. The predicted tendency of the harmonic confinement to *lower* the threshold of the steady-state formation compared to the trap-free case, agrees with the numerically calculated cut-off values in Fig. 4. Above the threshold, the harmonic trap leads, for the same parameters

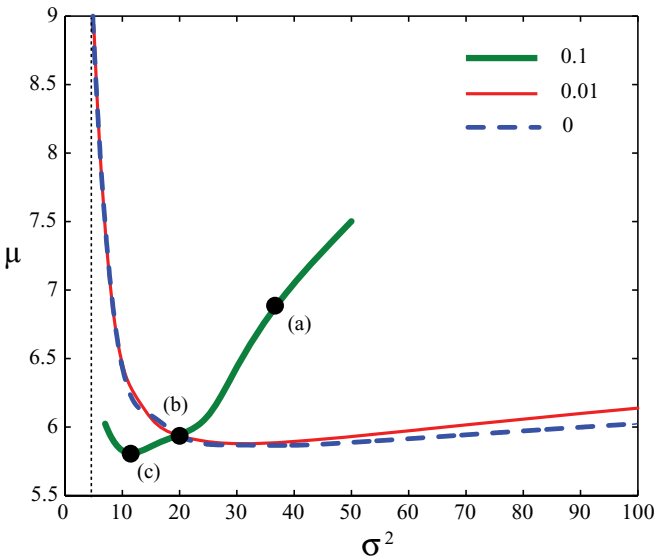

FIG. 5. (Color online) Dependence $\mu(\sigma^2)$ for the ground state $m = 0$ achieved at $\bar{P}_0 = 5$ without and with a harmonic trapping potential $U(r) = U_0^2 r^2$ with $U_0^2 = 0$ (dashed), $U_0^2 = 0.01$ (solid), and $U_0^2 = 0.01$ (thick solid line). The vertical dotted line marks the cut-off value of the pump width for the trap-free ground state given by the linear limit expression (14) resolved with respect to σ^2. Marked points [(a)–(c)] correspond to the condensate profiles shown in Fig. 6.

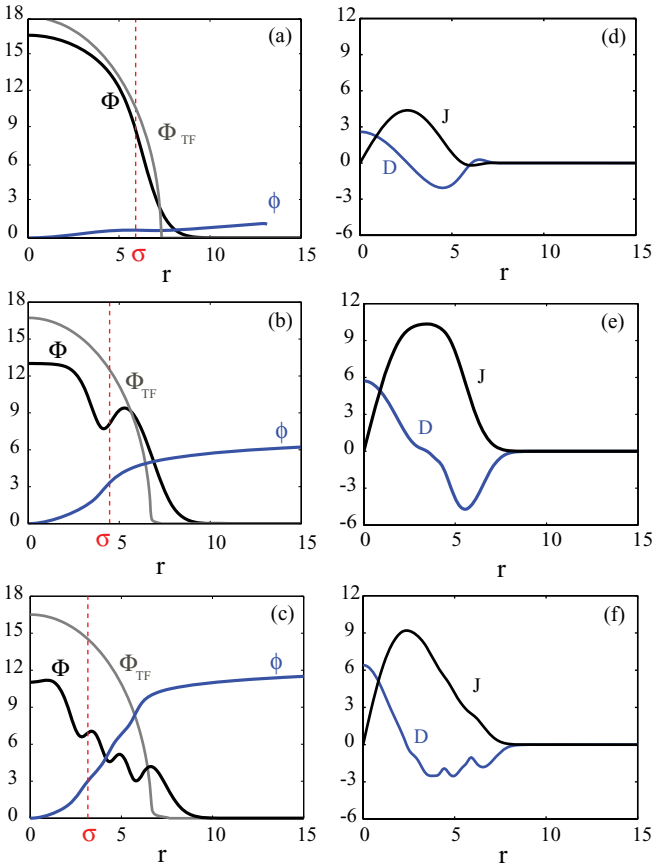

FIG. 6. (Color online) Radial shapes of the condensate ground states in the harmonically trapped case for $U_0^2 = 0.1$, $\bar{P}_0 = 5$ and the width of the pump spot σ^2 corresponding to the points marked in Fig. 5. (a)–(c) Both amplitude, $\Phi(r)$, and phase, $\phi(r)$, are shown in comparison to the condensate profile obtained in the Thomas-Fermi approximation, $\Phi_{\rm TF}$ (gray). (d)–(f) Profiles of the radial flux J and its divergence D (scaled up by the factor of 10) for the ground states shown in the panels (a)–(c).

of the pump, to the formation of the steady-state BEC with stronger spatial localization and higher peak density, as can be seen from comparison of Figs. 3(a) and 3(b).

For a fixed strength of the harmonic confinement, the width of the pump spot determines different trapping regimes. Intuitively, for an excitation spot much wider than the trap, the limiting behavior should be described by a homogeneous pump approximation $P(r) \approx P_0$ [15,20]. In the opposite regime of a narrow excitation spot, the limiting behavior should be close to that of a free condensate. Contrary to this intuitive picture, the dependence of the chemical potential μ on the width of the excitation spot σ^2 calculated numerically shows dramatic differences for trapped and free condensates (Fig. 5). Most notably, a trapped condensate displays well-pronounced bistability, whereby both narrow and wide pumps can support two different steady states with the same energy. In addition, the condensate density profiles are strongly spatially modulated (see Fig. 6). This is due to the presence of two competing spatial scales. One of them, $\sim\sigma$, is defined by the pump, and the other one, $\sim r_{\rm TF}$, is defined by the trapping potential and is given by the characteristic radius of the wave function in the Thomas-Fermi limit. The latter is obtained by neglecting both phase and density gradients in Eqs. (10), as the solution to the equation:

$$U_0^2 r_{\rm TF}^2 + \frac{\gamma_c g_R}{R}\bar{P}_0 \exp\left(-\frac{r_{\rm TF}^2}{\sigma^2}\right) = \mu. \qquad (15)$$

In the regime of a wide pump, the condensate density can be reasonably well approximated by the radially symmetric Thomas-Fermi profile with the radius $r_{\rm TF}$ given by Eq. (15), as can be seen in Fig. 6(a). In this regime, the ground state in the form of a dissipative soliton becomes dynamically unstable with respect to azimuthal perturbations for $\bar{P}_0 \gg 1$, as established in [20]. There it was shown that this instability can lead to rotational symmetry breaking whereby multiple vortex states enter the condensate.

For a very narrow pump, $\sigma^2 \ll r_{\rm TF}^2$, the Thomas-Fermi radius exactly coincides with the well-known expression for a conservative BEC with repulsive interparticle interactions in a harmonic trapping potential: $r_{\rm TF}^0 = \sqrt{\mu/U_0^2}$. In our numerical simulations we find that $r_{\rm TF} \approx r_{\rm TF}^0$ for a wide range of values $\sigma < r_{\rm TF}$. In this parameter regime the condensate density profile strongly deviates from the Thomas-Fermi profile [Figs. 6(b) and 6(c)], as neither phase nor density gradients can be neglected. The condensate experiences strong modulations of density with a notable density dip along the line $D = 0$ separating the regions of loss and gain. The condensate peak density is also damped as the pump narrows down and the dip at $r = 0$ appears for the values of σ corresponding to the negative value of q_- in (8). We note that the point (b) in Fig. 5 corresponds to $q_- = 0$ for $U_0^2 = 0.1$. Under the

conditions of a strong ($\bar{P}_0 \gg 1$) narrow pump the steady state is dynamically unstable and exhibits strong peak density oscillations.

V. SINGLE VORTEX STATE

Spatially localized dissipative vortices are similarly found as higher-order steady states of the system with $m \neq 0$ [21], both in a trap-free and harmonically trapped polariton BEC. Numerically, the system relaxes to a single steady-state vortex when a phase factor $\exp(im\theta)$ is imprinted onto a condensate "seed" at the initial stages of evolution. The dependence of the chemical potential μ on the pump amplitude $\bar{P}_0$ is plotted in Fig. 7 for a vortex with $m = 1$. As expected, the chemical potential and the cutoff for this excited state are higher than those of the ground state of the trap-free condensate. In contrast, in a harmonic potential the vortex and the ground state become nearly degenerate (see Fig. 7).

The global phase of the vortex is imposed not only by the vorticity but also by the nonzero flux, and therefore depends on both azimuthal (θ) and radial (r) coordinates. Using the expression (8) for the radial dependence of the phase near the vortex core, we find that the lines of the constant phase follow a spiral trajectory described by the equations

$$x_s(\theta) = \sqrt{\theta/q_+}\cos\theta, \quad y_s(\theta) = \sqrt{\theta/q_+}\sin\theta.$$

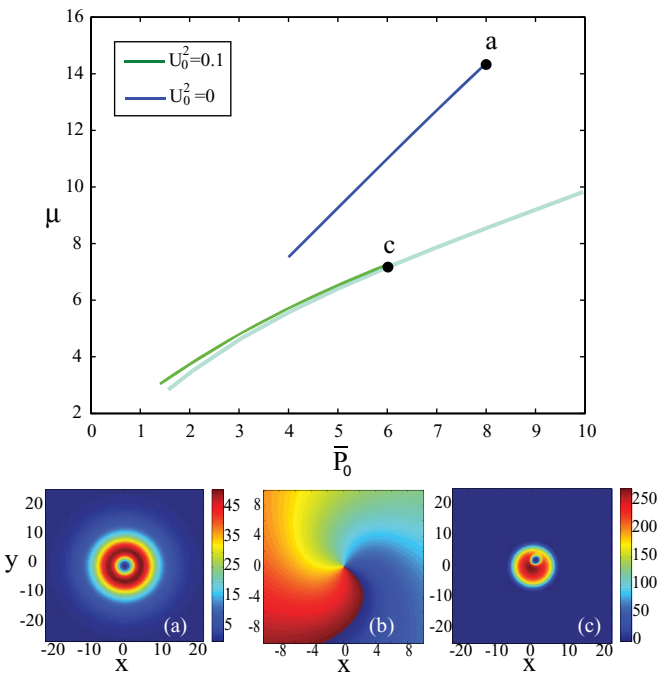

FIG. 7. (Color online) Top: Dependence $\mu(\bar{P}_0)$ for the vortex state $m = 1$ without and with the harmonic trapping potential $U(r) = U_0^2 r^2$ for $\sigma^2 = 30$. The semitransparent line indicates the corresponding dependence for a trapped $m = 0$ state from Fig. 4. Bottom: (a) Condensate density and (b) phase for a dynamically unstable $m = 1$ stationary vortex state in a trap-free condensate at $\bar{P}_0 = 8$. (c) Metastable rotating vortex state supported by a harmonic trap ($U_0^2 = 0.1$) at $\bar{P}_0 = 6$.

This spiral phase structure is shown in Fig. 7(b) for the numerically found localized vortex state in Fig. 7(a), without the trapping potential. It is a signature of the polariton BEC vortex observed in the experiments [2], and also appears as a characteristic feature of vortex states in other dissipative systems [17,22,23].

The ground state ($m = 0$) of the polariton condensate is dynamically stable in the absence of a trap. In contrast, we find that a single vortex created in a localized steady-state BEC by phase imprinting is dynamically unstable and, in the absence of potential, spirals out of the condensate, as predicted for the case of trapped dissipative BEC of alkali atoms [14,24]. As can be seen from comparison of Figs. 4 and 7, the addition of a stationary (i.e., nonrotating) harmonic potential dramatically modifies the threshold of the optical pumping required to sustain a steady state of a polariton BEC with an angular momentum and leads to the possibility of a long-term survival of the vortex in the form of an eccentric rotating state shown in Fig. 7(c). The detailed study of the stabilizing effect of the trapping potential on the vortex dynamics and the dynamics near the onset of rotational symmetry breaking [20] is beyond the scope of this study. However, we have confirmed that a wide pump (corresponding to small density gradients in the harmonic trap) tends to stabilize the vortex state.

VI. CONCLUSIONS

We have characterized the 2D stationary regime of the polariton BEC in the framework of an open-dissipative Gross-Pitaevskii model coupled to an exciton reservoir and described, both analytically and numerically, properties of the ground and excited states (vortices) depending on the pump and trapping parameters. We have shown that the spatial localization of the condensate, even in the absence of a trapping potential, is supported by the balance of the internal superfluid flows established by an inhomogeneous nonlinear gain due to optical pump and linear loss due to the decay of the polaritons. The ground state of the condensate can therefore be described as a *continuously self-defocusing dissipative soliton*. We have also investigated localized dissipative vortex states and have shown that they can display metastable behavior in nonrotating trapping potentials.

Finally, we note that the open-dissipative model with the inhomogeneous pump used here and successfully employed for theoretical description of experiments with microcavity polaritons, has many similarities to optical systems with localized gain landscapes [13,22]. These and similar studies suggest that the 2D stationary regime of polariton BEC can potentially display a rich variety of localized states which are not exhausted by radially symmetric configurations. In particular, the experiments with polariton BEC excited by the elliptical optical pump have demonstrated pattern formation due to the appearance of standing waves [25]. Furthermore, the recent experiment with polariton BECs created by two pump spots [26] demonstrates novel possibilities arising from *interaction of two dissipative solitons with variable separation*. The clear understanding of the structure of phase gradients underpinning the existence of steady-state polariton condensates presented in our work enables us to gain immediate insight into the

properties and outcomes of such interactions. The possibility to create a rich variety of localized states by varying the spatial properties of the off-resonant optical pump are currently under investigation and will be reported elsewhere.

ACKNOWLEDGMENT

This work was supported by the Australian Research Council (ARC).

[1] J. Kasprzak, M. Richard, S. Kundermann, A. Baas, P. Jeambrun, J. M. J. Keeling, F. M. Marchetti, M. H. Szymańska, R. André, J. L. Staehli, V. Savona, P. B. Littlewood, B. Deveaud, and Le Si Dang, Nature (London) **443**, 409 (2006).

[2] K. G. Lagoudakis, M. Wouters, M. Richard, A. Baas, I. Carusotto, R. Andre, Le Si Dang, and B. Deveaud-Plédran, Nat. Phys. **4**, 706 (2008).

[3] A. Amo, S. Pigeon, D. Sanvitto, V. G. Sala, R. Hivet, I. Carusotto, F. Pisanello, G. Leménager, R. Houdré, E. Giacobino, C. Ciuti, and A. Bramati, Science **332**, 1167 (2011).

[4] G. Roumpos, M. D. Fraser, A. Löffler, S. Höfling, A. Forchel, and Y. Yamamoto, Nat. Phys. **7**, 129 (2011).

[5] G. Nardin, G. Grosso, Y. Léger, B. Piętka, F. Morier-Genoud, and B. Deveaud-Plédran, Nat. Phys. **7**, 635 (2011).

[6] O. A. Egorov, A. V. Gorbach, F. Lederer, and D. V. Skryabin, Phys. Rev. Lett. **105**, 073903 (2010).

[7] N. N. Rosanov, Nature Photon. **6**, 6 (2012).

[8] M. Sich, D. N. Krizhanovskii, M. S. Skolnik, A. V. Gorbach, R. Hartley, D. V. Skryabin, E. A. Cerda-Méndez, K. Biermann, R. Hey, and P. V. Santos, Nature Photon. **6**, 50 (2012).

[9] H. Pu, L. O. Baksmaty, W. Zhang, N. P. Bigelow, and P. Meystre, Phys. Rev. A **67**, 043605 (2003); B. Eiermann, Th. Anker, M. Albiez, M. Taglieber, P. Treutlein, K.-P. Marzlin, and M. K. Oberthaler, Phys. Rev. Lett. **92**, 230401 (2004); E. A. Ostrovskaya and Yu. S. Kivshar, Opt. Express **12**, 19 (2004).

[10] M. Wouters and I. Carusotto, Phys. Rev. Lett. **99**, 140402 (2007).

[11] R. Balili, V. Hartwell, D. W. Snoke, L. Pfeiffer, and K. West, Science **316**, 1007 (2007).

[12] A. E. Siegman, J. Opt. Sov. Am. A **20**, 1617 (2003).

[13] D. A. Zezyulin, Y. V. Kartashov, and V. V. Konotop, Opt. Lett. **36**, 1200 (2011).

[14] A. L. Fetter and A. A. Svidzinsky, J. Phys.: Condens. Matter **13**, R135 (2001).

[15] M. Wouters, I. Carusotto, and C. Ciuti, Phys. Rev. B **77**, 115340 (2008).

[16] A. S. Desyatnikov, Yu. S. Kivshar, and L. Torner, Prog. Opt. **47**, 291 (2005).

[17] N. N. Rozanov, S. V. Fedorov, and A. N. Shatsev, JETP **98**, 427 (2003).

[18] M. Edwards and K. Burnett, Phys. Rev. A **51**, 1382 (1995).

[19] A. Ankiewicz, N. Devine, N. Akhmediev, and J. M. Soto-Crespo, Phys. Rev. A **77**, 033840 (2008).

[20] J. Keeling and N. G. Berloff, Phys. Rev. Lett. **100**, 250401 (2008).

[21] Yu. S. Kivshar, T. J. Alexander, and S. K. Turitsyn, Phys. Lett. A **4**, 225 (2001).

[22] V. E. Lobanov, Y. V. Kartashov, V. A. Vysloukh, and L. Torner, Opt. Lett. **36**, 85 (2011).

[23] A. M. Sergeev and V. I. Petviashvili, Dokl. Akad. Nauk SSSR **276**, 1380 (1984) [Sov. Phys. Dokl. **29**, 493 (1984)]; L.-C. Crasovan, B. A. Malomed, and D. Mihalache, Phys. Rev. E **63**, 016605 (2000).

[24] P. O. Fedichev and G. V. Shlyapnikov, Phys. Rev. A **60**, R1779 (1999).

[25] F. Manni, K. G. Lagoudakis, T. C. H. Liew, R. André, and B. Deveaud-Plédran, Phys. Rev. Lett. **107**, 106401 (2011).

[26] G. Tosi, G. Christmann, N. G. Berloff, P. Tsotsis, T. Gao, Z. Hatzopoulos, P. G. Savvidis, and J. J. Baumberg, Nat. Phys. **8**, 190 (2012).